On the Influence of Chirp Correlations upon OCFDM's Data Rate

Túlio F. Moreira, Wallace A. Martins, and Moisés V. Ribeiro

***Abstract*— This paper takes the first step in exploiting the correlations between chirps to increase the data rate of orthogonal chirp-frequency division multiplexing (OCFDM) systems. To do so, the OCFDM system model is first revisited, and then its achievable data rate is written as a function of the correlated-signal-to-noise ratio (cSNR) matrix. A power allocation problem, termed optimal allocation (OA), is then formulated targeting data-rate maximization, resulting in a concave optimization problem, which can be readily solved via semi-definite programming. The numerical results show that chirp correlations can significantly boost data rate. Notably, under uniform power allocation, the performance becomes independent of the way the frequency tilings are defined, unlike the behavior under OA. In addition, OA tends to distribute power evenly among chirps within the same frequency tiling, termed voice, while still allowing flexibility across different voices, paralleling previously reported results when disregarding chirp correlations. Overall, the findings suggest that exploiting chirp correlations can play a key role in improving OCFDM's performance.**

***Keywords*— correlation, multichirp, power allocation.**

I. Introduction

The orthogonal frequency division multiplexing (OFDM) has been the backbone of the physical (PHY)-layer of several communication systems for the past decades, being present, for instance, in Long-Term Evolution (LTE) and 5G [1]. Its ability to divide the bandwidth into multiple subcarriers makes OFDM highly efficient for data transmission, especially when facing frequency-selective channels and when resource allocation is properly performed. Yet, the research community continues to search for new waveforms that can address OFDM's limitations, while remaining capable of delivering the same benefits.

Proposed in 2016, the orthogonal chirp division multiplexing (OCDM) [2], a chirp spread spectrum (CSS)-based multicarrier modulation, is a promising alternative waveform. This technique employs orthogonal chirps to transmit data and attains superior bit-error rate (BER) performance compared to OFDM in certain scenarios [2]. Furthermore, it exhibits greater robustness to various types of interference, including those caused by a too-short cyclic prefix (CP) [3], symbol timing offset (STO), carrier frequency offset (CFO), and other impairments in the frequency band [4], [5]. However, this also limits the signal's flexibility in both time and frequency domains, potentially reducing its data rate and introducing challenges for implementing multiple access techniques [6]. Hence, one can state that OFDM and OCDM excel in different aspects of communications, the former being more flexible and presenting a higher data rate whereas the latter being more robust and less data rate.

In this context, the orthogonal chirp-frequency division multiplexing (OCFDM) [7], [8] has been recently introduced as a new waveform that incorporates both CSS and frequency division characteristics, effectively merging the principles of OFDM and OCDM. The authors in [7] showed that OCFDM replicates key features of both OFDM and OCDM, namely high data rates, low BER, and strong robustness to interference. In addition, OCFDM offers flexibility in its design, allowing trade-offs between data rate and BER. With respect to the normalized signal-to-noise ratio (nSNR) in OCFDM, it was shown that chirps within the same *voice*—a portion of the available bandwidth comprised of one or more chirps—share identical nSNR values, whereas chirps in other voices exhibit different nSNR values, enabling the application of resource allocation techniques across voices, which is impossible in the OCDM.

However, *the extensive analyses conducted in [7] overlooked the correlations between different chirps within the same voice*—a factor that could potentially be exploited to enhance both BER and data rate. To fill in this gap, this paper aims to investigate the impact of the correlation between chirps comprising the voices on the achievable data rate in OCFDM systems. To achieve that, the paper first describes OCFDM's achievable data rate when chirp correlations are factored in. The resulting expression—see (13)—differs from expression (45) in [7], wherein fully parallel channels were considered for the sake of mathematical simplicity. Building on that, a power allocation problem is formulated as a constrained concave optimization problem, which can be tackled by off-the-shelf solvers. The resulting achievable data rate is numerically studied considering different frequency tilings and different power allocation methods. Thus, this paper is an initial study regarding the potential benefits that such chirp correlations may yield.

A. Organization

The remainder of this paper is organized as follows: Section II revisits the OCFDM technique and presents its signal model. Section III presents the correlated-signal-to-noise ratio (SNR), the achievable data rate, and the underlying optimization problem for power allocation. Section IV describes the

This research was supported in part by Coordenação de Aperfeiçoamento de Pessoal de Nível Superior (CAPES) under Grant 001, Conselho Nacional de Desenvolvimento Científico e Tecnológico (CNPq) under grants 445958/2024-3 and 314741/2020-8, and Fundação de Amparo à Pesquisa do Estado de Minas Gerais (FAPEMIG) under grant APQ-04623-22.

Túlio F. Moreira and Moisés V. Ribeiro are with the Electrical Engineering Department, Federal University of Juiz de Fora, Juiz de Fora, MG 36036-900, Brazil, (e-mail: tuliofmoreira3@gmail.com, moises.ribeiro@ufjf.br)

Wallace A. Martins is with the Fédération ENAC ISAE-SUPAERO ONERA, Université de Toulouse, France (e-mail: wallace.martins@isae-supaero.fr).

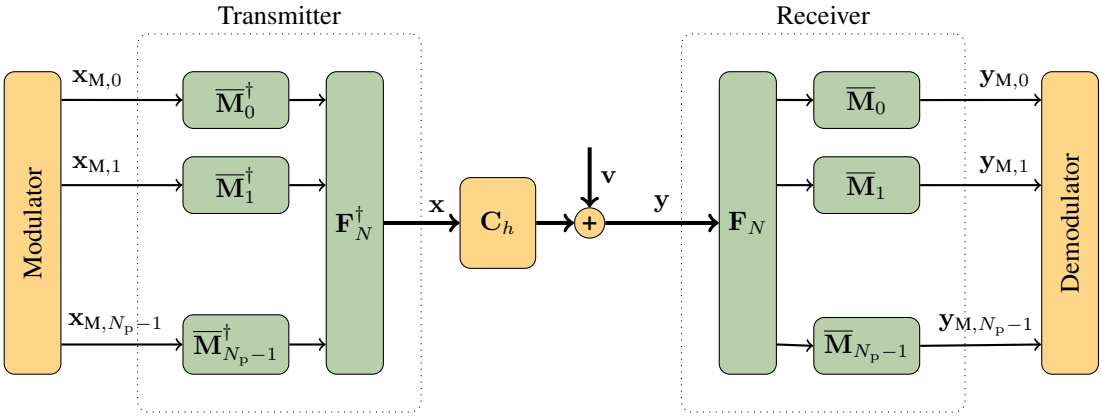

Fig. 1: The OCFDM block diagram.

numerical analysis focusing on the achievable data rate and its optimization. Section V outlines the concluding remarks.

B. Notation

In this paper, $\mathbb{E}\{\cdot\}$ denotes the expectation operator, whereas $(\cdot)^{\mathrm{T}}$, $(\cdot)^*$, and $(\cdot)^\dagger$ denote the transpose, conjugate, and conjugate transpose operators, respectively. Moreover, $\mathbf{0}_{a\times b}$ stands for an $(a \times b)$-size matrix of zeros and $\mathbf{I}_c$ is an c-size identity matrix. $\mathbf{F}_N \in \mathbb{C}^{N\times N}$ is the N-size normalized discrete Fourier transform (DFT) matrix such that the element in the k^{th} row and n^{th} column is equal to $F_{N,k,n} = \exp(-\mathrm{j}2\pi kn/N)/\sqrt{N}$ with $N = 2^d$ for $d \in \mathbb{N}^*$. Also, given $a_0 \in \mathbb{R}$, $\lfloor a_0 \rfloor = \max\{m \in \mathbb{Z} \mid m \leq a_0\}$, $\lceil a_0 \rceil = \min\{m \in \mathbb{Z} \mid m \geq a_0\}$, and given $b_0, c_0 \in \mathbb{Z}$, an interval of integers can be defined as $[b_0, c_0] = \{x \in \mathbb{Z} \mid b_0 \leq x \leq c_0\}$. Lastly, $\bigoplus$ is the direct sum operator.

II. System Model

In this section, the system model for an OCFDM-based system is detailed. This communication system relies on the discrete modular chirp transform (DMCT) [7], [8], which is the transform responsible for creating chirps within a predefined frequency division pattern (tiling), hereafter referred to as *geometry*—for further details regarding geometry in OCFDM, see Sections II.A and III.B of [7]. The DMCT matrix, $\mathbf{M}$, is given by

$$\mathbf{M} = \overline{\mathbf{M}}\mathbf{F}_N, \tag{1}$$

wherein $\overline{\mathbf{M}} \in \mathbb{C}^{N\times N}$ is a block-diagonal matrix equal to

$$\begin{aligned}\overline{\mathbf{M}} &= \begin{bmatrix} \overline{\mathbf{M}}_0 & \mathbf{0}_{\beta_0\times\beta_1} & \cdots & \mathbf{0}_{\beta_0\times\beta_{N_\mathrm{p}-1}} \\ \mathbf{0}_{\beta_1\times\beta_0} & \overline{\mathbf{M}}_1 & \cdots & \mathbf{0}_{\beta_1\times\beta_{N_\mathrm{p}-1}} \\ \vdots & \vdots & \ddots & \vdots \\ \mathbf{0}_{\beta_{N_\mathrm{p}-1}\times\beta_0} & \mathbf{0}_{\beta_{N_\mathrm{p}-1}\times\beta_1} & \cdots & \overline{\mathbf{M}}_{N_\mathrm{p}-1} \end{bmatrix} \\ &= \bigoplus_{p=0}^{N_\mathrm{p}-1} \overline{\mathbf{M}}_p \end{aligned} \tag{2}$$

with N_p being the number of voices. The matrix $\overline{\mathbf{M}}_p \in \mathbb{C}^{\beta_p\times\beta_p}$, $p \in [0, N_\mathrm{p}-1]$, is in charge of the digital processing of the chirps related to the p^{th} voice and is equal to $\overline{\mathbf{M}}_p = \mathbf{\Lambda}_{\mathrm{PS},p}\mathbf{F}^\dagger_{\beta_p}\mathbf{\Lambda}_{\mathrm{ZC},p}$, with the matrices $\mathbf{\Lambda}_{\mathrm{PS},p}$ and $\mathbf{\Lambda}_{\mathrm{ZC},p}$ being diagonal matrices with their respective m^{th} and k^{th} diagonal element equal to $\Lambda_{\mathrm{PS},p,m,m} = \exp(\mathrm{j}2\pi\tau_{p,m}(\nu_p - \lfloor\beta_p/2\rfloor)/\beta_p)$ and $\Lambda_{\mathrm{ZC},p,k,k} = \exp(-\mathrm{j}\pi k^2/\beta_p)$. The parameters β_p, ν_p, and $\boldsymbol{\tau}_p$ are related to the geometry and describe the size, central frequency index, and time indexes of the p^{th} voice, respectively [7]. The case in which $\mathbf{\Lambda}_{\mathrm{PS},p} = \mathbf{I}_{\beta_p}$ characterizes what is called a *regular geometry*, wherein $\overline{\mathbf{M}}_p$ simplifies to

$$\overline{\mathbf{M}}_p = \mathbf{F}^\dagger_{\beta_p}\mathbf{\Lambda}_{\mathrm{ZC},p}. \tag{3}$$

As the DMCT is a unitary transform, the inverse discrete modular chirp transform (IDMCT) is given by $\mathbf{M}^\dagger$.

Fig. 1 depicts the block diagram of an OCFDM system, already considering CP inclusion of length $L_{\mathrm{cp}} \geq L_h - 1$, wherein L_h is the length of the discrete-time channel model. The vector of modulated symbols, $\mathbf{x}_\mathrm{M} = [\mathbf{x}^{\mathrm{T}}_{\mathrm{M},0}\ \mathbf{x}^{\mathrm{T}}_{\mathrm{M},1}\ \cdots\ \mathbf{x}^{\mathrm{T}}_{\mathrm{M},N_\mathrm{p}-1}]^{\mathrm{T}} \in \mathbb{C}^{N\times 1}$ is digitally processed by the transmitter, by applying the IDMCT, thus yielding

$$\begin{aligned}\mathbf{x} &= \mathbf{F}^\dagger_N\overline{\mathbf{M}}^\dagger\mathbf{x}_\mathrm{M} \\ &= \mathbf{F}^\dagger_N[(\overline{\mathbf{M}}^\dagger_0\mathbf{x}_{\mathrm{M},0})^{\mathrm{T}}\ \cdots\ (\overline{\mathbf{M}}^\dagger_{N_\mathrm{p}-1}\mathbf{x}_{\mathrm{M},N_\mathrm{p}-1})^{\mathrm{T}}]^{\mathrm{T}},\end{aligned} \tag{4}$$

with $\mathbf{x}_{\mathrm{M},p} = [x_{\mathrm{M},\mathrm{lb}_p}\ x_{\mathrm{M},\mathrm{lb}_p+1}\ \cdots\ x_{\mathrm{M},\mathrm{ub}_p}]^{\mathrm{T}} \in \mathbb{C}^{\beta_p\times 1}$ being the vector of signals in the p^{th} voice, $\mathrm{lb}_p = \nu_p - \lfloor\beta_p/2\rfloor$, and $\mathrm{ub}_p = \nu_p + \lfloor\beta_p/2\rfloor$. After passing through the multipath wireless channel, $\mathbf{h} \in \mathbb{C}^{L_h\times 1}$, and being disturbed by the additive noise vector $\mathbf{v} \in \mathbb{C}^{N\times 1}$, the vector $\mathbf{y}$ of symbols after the CP removal is equal to

$$\mathbf{y} = \mathbf{C}_h\mathbf{x} + \mathbf{v}, \tag{5}$$

in which $\mathbf{C}_h \in \mathbb{C}^{N\times N}$ denotes the equivalent channel circulant matrix. Assuming perfect synchronization, at the receiver side, the DMCT is applied to $\mathbf{y}$, resulting in the vector $\mathbf{y}_\mathrm{M}$, given by

$$\begin{aligned}\mathbf{y}_\mathrm{M} &= \overline{\mathbf{M}}\mathbf{F}_N\mathbf{y} \\ &= \overline{\mathbf{M}}\mathbf{F}_N\mathbf{C}_h\mathbf{F}^\dagger_N\overline{\mathbf{M}}^\dagger\mathbf{x}_\mathrm{M} + \overline{\mathbf{M}}\mathbf{F}_N\mathbf{v} \\ &= \overline{\mathbf{M}}\mathbf{\Lambda}_{h_\mathrm{F}}\overline{\mathbf{M}}^\dagger\mathbf{x}_\mathrm{M} + \overline{\mathbf{M}}\mathbf{F}_N\mathbf{v}.\end{aligned} \tag{6}$$

with $\mathbf{\Lambda}_{h_{\mathrm{F}}^u}$ being a diagonal matrix in which its diagonal elements are obtained from the vector $\mathbf{h}_{\mathrm{F}}^u = \sqrt{N}\mathbf{F}_N\mathbf{h}_{\mathrm{z}}^u \in \mathbb{C}^{N\times 1}$, with $\mathbf{h}_{\mathrm{z}}^u = [\mathbf{h}^{u\mathrm{T}}\ \mathbf{0}_{(N-L_{h^u})\times 1}^{\mathrm{T}}]^{\mathrm{T}}$. Applying (3) to (6) and using the commutation property of diagonal matrices, one can obtain

$$\begin{aligned}\mathbf{y}_{\mathrm{M}} &= \left(\bigoplus_{p=0}^{N_{\mathrm{p}}-1}\mathbf{F}_{\beta_p}^{\dagger}\mathbf{\Lambda}_{h_{\mathrm{F}},p}\mathbf{F}_{\beta_p}\right)\mathbf{x}_{\mathrm{M}} + \left(\bigoplus_{p=0}^{N_{\mathrm{p}}-1}\mathbf{F}_{\beta_p}^{\dagger}\mathbf{\Lambda}_{\mathrm{ZC},p}\right)\mathbf{v}_{\mathrm{F}}\\ &= \left(\bigoplus_{p=0}^{N_{\mathrm{p}}-1}\mathbf{C}_{h_{\mathrm{M}},p}\right)\mathbf{x}_{\mathrm{M}} + \left(\bigoplus_{p=0}^{N_{\mathrm{p}}-1}\mathbf{F}_{\beta_p}^{\dagger}\mathbf{\Lambda}_{\mathrm{ZC},p}\right)\mathbf{v}_{\mathrm{F}}\\ &= [\mathbf{y}_{\mathrm{M},0}^{\mathrm{T}}\ \mathbf{y}_{\mathrm{M},1}^{\mathrm{T}}\ \cdots\ \mathbf{y}_{\mathrm{M},N_{\mathrm{p}}-1}^{\mathrm{T}}]^{\mathrm{T}},\end{aligned} \tag{7}$$

in which $\mathbf{\Lambda}_{h_{\mathrm{F}},p} \in \mathbb{C}^{\beta_p\times\beta_p}$ is a diagonal matrix with elements equal to $\Lambda_{h_{\mathrm{F}},k,k}$, $k \in [\mathrm{lb}_p, \mathrm{ub}_p]$ and

$$\mathbf{y}_{\mathrm{M},p} = \mathbf{C}_{h_{\mathrm{M}},p}\mathbf{x}_{\mathrm{M}} + \mathbf{F}_{\beta_p}^{\dagger}\mathbf{\Lambda}_{\mathrm{ZC},p}\mathbf{v}_{\mathrm{F}}. \tag{8}$$

III. Correlated-SNR: Data Rate and Its Maximization

In order to assess OCFDM's data rate, let us first rewrite (7) in terms of random vectors so that we may derive the main statistical moments, *i.e.*, mean and covariance, of the desired signals and noise, while still keeping a deterministic channel model. Hence, vector $\mathbf{y}_{\mathrm{M}}$ in (7) can be seen as a realization of the random vector

$$\begin{aligned}\boldsymbol{\mathcal{Y}}_{\mathrm{M}} &= \left(\bigoplus_{p=0}^{N_{\mathrm{p}}-1}\mathbf{C}_{h_{\mathrm{M}},p}\right)\boldsymbol{\mathcal{X}}_{\mathrm{M}} + \left(\bigoplus_{p=0}^{N_{\mathrm{p}}-1}\mathbf{F}_{\beta_p}^{\dagger}\mathbf{\Lambda}_{\mathrm{ZC},p}\right)\mathbf{F}_N\boldsymbol{\mathcal{V}}\\ &= \widehat{\boldsymbol{\mathcal{X}}}_{\mathrm{M}} + \boldsymbol{\mathcal{V}}_{\mathrm{M}},\end{aligned} \tag{9}$$

wherein $\boldsymbol{\mathcal{V}}$ is normally distributed with mean $\boldsymbol{\mu}_{\boldsymbol{\mathcal{V}}} = \mathbf{0}_{N\times 1}$ and covariance matrix $\mathbf{\Sigma}_{\boldsymbol{\mathcal{V}}} = P_v\mathbf{I}_N$, with P_v being the noise power. This makes $\boldsymbol{\mathcal{V}}_{\mathrm{M}}$ also be described as a zero-mean Gaussian vector with covariance matrix $\mathbf{\Sigma}_{\boldsymbol{\mathcal{V}}_{\mathrm{M}}} = P_v\mathbf{I}_N$. Moreover, $\boldsymbol{\mathcal{X}}_{\mathrm{M}}$ is the vector containing independent random variables $\mathcal{X}_{\mathrm{M},n}$, $n \in [0, N-1]$, with its mean being $\boldsymbol{\mu}_{\boldsymbol{\mathcal{X}}_{\mathrm{M}}} = \mathbf{0}_{N\times 1}$ and covariance matrix $\mathbf{\Sigma}_{\boldsymbol{\mathcal{X}}_{\mathrm{M}}} = \mathbf{\Lambda}_{P_x} \in \mathbb{R}_+^{N\times N}$, a diagonal matrix with elements given by the power of the n^{th} random signal. Finally, $\widehat{\boldsymbol{\mathcal{X}}}_{\mathrm{M}} = (\bigoplus_{p=0}^{N_{\mathrm{p}}-1}\mathbf{C}_{h_{\mathrm{M}},p})\boldsymbol{\mathcal{X}}_{\mathrm{M}}$ represents the random vector after processed by the effective channel of each voice, whose mean is given by

$$\begin{aligned}\boldsymbol{\mu}_{\widehat{\boldsymbol{\mathcal{X}}}_{\mathrm{M}}} &= \left(\bigoplus_{p=0}^{N_{\mathrm{p}}-1}\mathbf{C}_{h_{\mathrm{M}},p}\right)\boldsymbol{\mu}_{\boldsymbol{\mathcal{X}}_{\mathrm{M}}}\\ &= \mathbf{0}_{N\times 1},\end{aligned} \tag{10}$$

and whose covariance matrix is given by

$$\begin{aligned}\mathbf{\Sigma}_{\widehat{\boldsymbol{\mathcal{X}}}_{\mathrm{M}}} &= \mathbb{E}\{(\widehat{\boldsymbol{\mathcal{X}}}_{\mathrm{M}} - \boldsymbol{\mu}_{\widehat{\boldsymbol{\mathcal{X}}}_{\mathrm{M}}})(\widehat{\boldsymbol{\mathcal{X}}}_{\mathrm{M}} - \boldsymbol{\mu}_{\widehat{\boldsymbol{\mathcal{X}}}_{\mathrm{M}}})^{\dagger}\}\\ &= \left(\bigoplus_{p=0}^{N_{\mathrm{p}}-1}\mathbf{C}_{h_{\mathrm{M}},p}\right)\mathbf{\Lambda}_{P_x}\left(\bigoplus_{p=0}^{N_{\mathrm{p}}-1}\mathbf{C}_{h_{\mathrm{M}},p}^{\dagger}\right)\\ &= \left(\bigoplus_{p=0}^{N_{\mathrm{p}}-1}\mathbf{C}_{h_{\mathrm{M}},p}\mathbf{\Lambda}_{P_x,p}\mathbf{C}_{h_{\mathrm{M}},p}^{\dagger}\right),\end{aligned} \tag{11}$$

in which $\mathbf{\Lambda}_{P_x,p} \in \mathbb{C}^{\beta_p\times\beta_p}$ is a diagonal matrix with diagonal elements $\Lambda_{P_x,k,k}$, $k \in [\mathrm{lb}_p, \mathrm{ub}_p]$. Thus, with the covariances of both signal and noise in the OCFDM context, we can derive the expression of the achievable data rate, considering the ideal case of Gaussian signaling. Considering a constellation-symbol period $1/B$, the achievable data rate is expressed as $R = B\overline{R}/(N + L_{\mathrm{cp}})$, with $\overline{R}$ given by [9]

$$\begin{aligned}\overline{R} &= \log_2\left(\det\left(\mathbf{I}_N + \mathbf{\Sigma}_{\boldsymbol{\mathcal{V}}_{\mathrm{M}}}^{-1}\mathbf{\Sigma}_{\widehat{\boldsymbol{\mathcal{X}}}_{\mathrm{M}}}\right)\right)\\ &= \log_2\left(\det\left(\mathbf{I}_N + P_v^{-1}\bigoplus_{p=0}^{N_{\mathrm{p}}-1}\mathbf{C}_{h_{\mathrm{M}},p}\mathbf{\Lambda}_{P_x}\mathbf{C}_{h_{\mathrm{M}},p}^{\dagger}\right)\right)\\ &= \log_2\left(\det\left(\bigoplus_{p=0}^{N_{\mathrm{p}}-1}\mathbf{I}_{\beta_p} + P_v^{-1}\mathbf{C}_{h_{\mathrm{M}},p}\mathbf{\Lambda}_{P_x}\mathbf{C}_{h_{\mathrm{M}},p}^{\dagger}\right)\right),\end{aligned} \tag{12}$$

wherein we name $\mathbf{\Sigma}_{\boldsymbol{\mathcal{V}}_{\mathrm{M}}}^{-1}\mathbf{\Sigma}_{\widehat{\boldsymbol{\mathcal{X}}}_{\mathrm{M}}}$ as SNR matrix. The above equation can be simplified by applying the determinant property of block diagonal matrices, which states that $\det(\bigoplus_{p=0}^{N_{\mathrm{p}}-1}\mathbf{A}_p) = \prod_{p=0}^{N_{\mathrm{p}}-1}\det(\mathbf{A}_p)$, reducing it to

$$\overline{R} = \sum_{p=0}^{N_{\mathrm{p}}-1}\log_2\left(\det\left(\mathbf{I}_{\beta_p} + P_v^{-1}\mathbf{C}_{h_{\mathrm{M}},p}\mathbf{\Lambda}_{P_x,p}\mathbf{C}_{h_{\mathrm{M}},p}^{\dagger}\right)\right). \tag{13}$$

Maximizing R is equivalent to maximizing $\overline{R}$ in (13). Therefore, we formulate the following optimization problem:

$$\begin{aligned}\underset{\mathbf{\Lambda}_{P_x,p}}{\text{maximize}}\quad & \sum_{p=0}^{N_{\mathrm{p}}-1}\log_2\left(\det\left(\mathbf{I}_{\beta_p} + P_v^{-1}\mathbf{C}_{h_{\mathrm{M}},p}\mathbf{\Lambda}_{P_x,p}\mathbf{C}_{h_{\mathrm{M}},p}^{\dagger}\right)\right)\\ \text{subject to}\quad & \sum_{p=0}^{N_{\mathrm{p}}-1}\mathrm{tr}\{\mathbf{\Lambda}_{P_x,p}\} = P_{\mathrm{T}},\\ & \Lambda_{P_x,p,k,k} \geq 0,\ \forall p \in [0, N_{\mathrm{p}}-1], \forall k \in [\mathrm{lb}_p, \mathrm{ub}_p],\end{aligned} \tag{14}$$

in which $P_{\mathrm{T}} > 0$ is the total transmission power.

The function $\det(\mathbf{A})$ is a log-concave function if $\mathbf{A}$ is a positive-definite matrix [10]. Thus, the objective function in problem (14) will be concave if $\mathbf{C}_{h_{\mathrm{M}},p}\mathbf{\Lambda}_{P_x,p}\mathbf{C}_{h_{\mathrm{M}},p}^{\dagger}$ is positive semi-definite $\forall p$. Indeed, this is the case, since $\mathbf{b}^{\dagger}\mathbf{C}_{h_{\mathrm{M}},p}\mathbf{\Lambda}_{P_x,p}\mathbf{C}_{h_{\mathrm{M}},p}^{\dagger}\mathbf{b} = \|\mathbf{\Lambda}_{P_x,p}^{1/2}\mathbf{C}_{h_{\mathrm{M}},p}^{\dagger}\mathbf{b}\|_2^2 \geq 0, \forall\mathbf{b} \in \mathbb{C}^{\beta_p\times 1}$. Therefore, the problem in (14) characterizes the maximization of a concave function with linear equality and inequality constraints, which means that there is only one optimal point and that disciplined convex programming can be used to solve it. In particular, this optimization problem can be straightforwardly adapted to be solved via semi-definite programming (SDP) [11].

IV. Numerical Analysis

This section describes the impact on the achievable data rate when the correlations of chirps comprising the voices of the OCFDM are considered. Such correlations are modeled by the off-diagonal entries of the SNR matrix $\mathbf{\Sigma}_{\boldsymbol{\mathcal{V}}_{\mathrm{M}}}^{-1}\mathbf{\Sigma}_{\widehat{\boldsymbol{\mathcal{X}}}_{\mathrm{M}}}$, herein called correlated-SNR (cSNR). The case studied in [7], where the correlations are disregarded, herein called uncorrelated-SNR (uSNR), will serve as a comparison baseline. Such baseline considers an SNR matrix given by a diagonal matrix with elements equal to the diagonal elements of $\mathbf{\Sigma}_{\boldsymbol{\mathcal{V}}_{\mathrm{M}}}^{-1}\mathbf{\Sigma}_{\widehat{\boldsymbol{\mathcal{X}}}_{\mathrm{M}}}$, *i.e.*, $\mathrm{diag}(\mathbf{\Sigma}_{\boldsymbol{\mathcal{V}}_{\mathrm{M}}}^{-1}\mathbf{\Sigma}_{\widehat{\boldsymbol{\mathcal{X}}}_{\mathrm{M}}})$. To this end, we focus on analyzing the

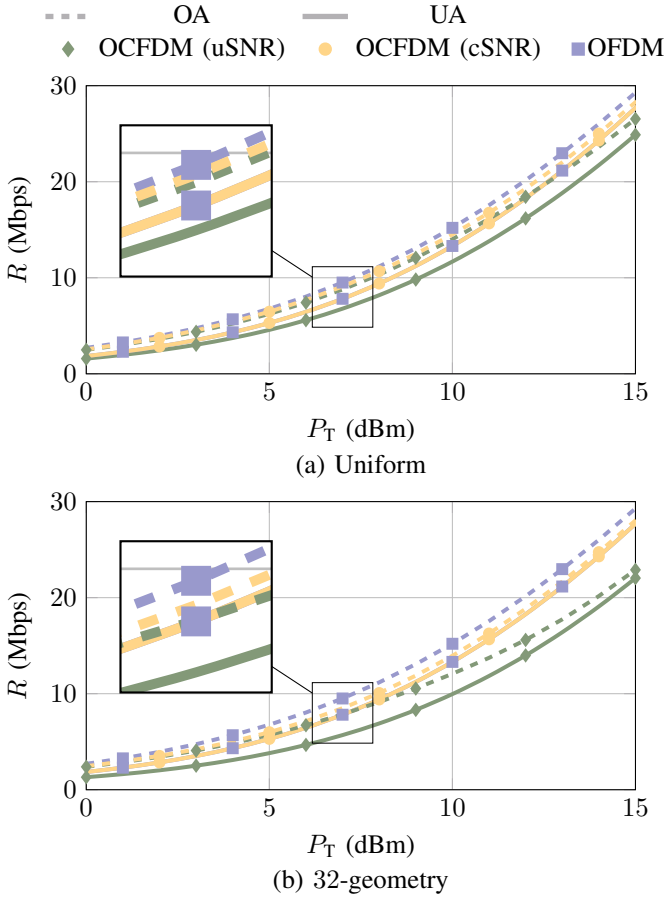

Fig. 2: $R \times P_{\mathrm{T}}$ comparison between OCFDM with uSNR and cSNR, while considering (a) Uniform and (b) 32-geometry.

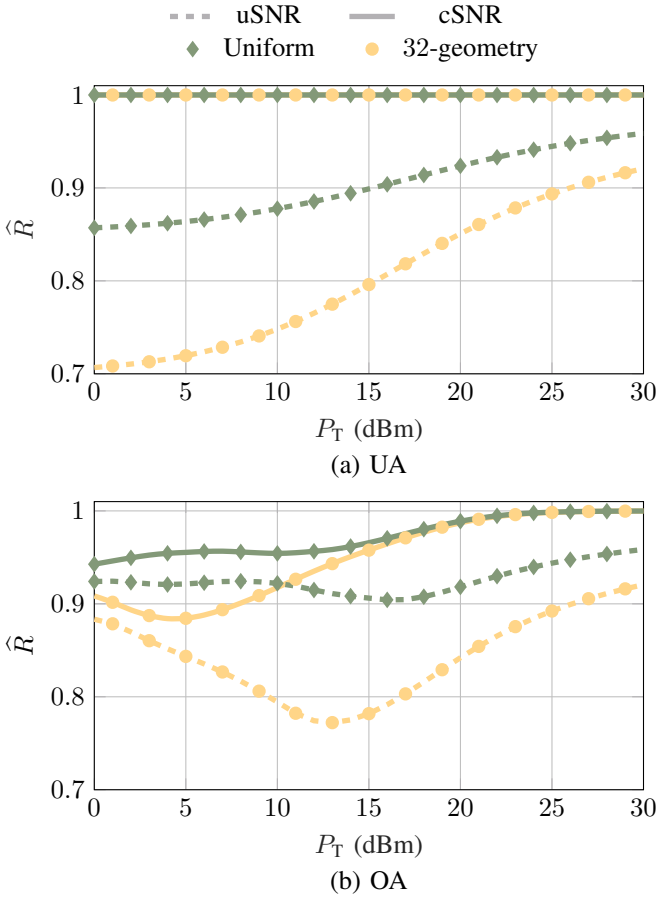

Fig. 3: $\widehat{R} \times P_{\mathrm{T}}$ comparison between OCFDM with uSNR and cSNR, while considering uniform and 32-geometry and (a) UA or (b) OA.

power allocated to each chirp and the resulting achievable data rate, including a comparison against OFDM, whose SNR matrix is given by $P_{\mathcal{V}}^{-1}|\mathbf{\Lambda}_{\boldsymbol{h}_{\mathrm{F}}}|^2\mathbf{\Lambda}_{P_x}$. Concerning the channel model, it was considered the IEEE 802.15.4a wireless channel model, covering small- and large-scale fading effects. We derived the small-scale considering the non-line-of-sight (NLOS) residential environment [12] while disregarding the frequency dependence of antennas. A bandwidth of $B = 20$ MHz around 2.4 GHz, with $N = 128$ chirps [13], was also considered. For large-scale fading, we assumed a log-distance path loss model without shadowing and a distance between transmitter and receiver equal to 7 m. The path loss exponent and the path loss at a reference distance were obtained from [14], considering the NLOS condition. The resulting channel had $L_h = 30$ in the time domain. Finally, optimal power allocation (OA) denotes the case in which the allocated power maximizes the achievable data rate—*i.e.,* the solution of problem (14)—and uniform power allocation (UA) denotes the case with an even distribution of power.

The numerical results of the achievable data rate are presented in two figures. Fig. 2 shows the curves of $R \times P_{\mathrm{T}}$ for UA and OA, whereas Fig. 3 depicts the curves of normalized achievable data rate $\widehat{R}$ by $P_{\mathrm{T}} \in [0, 15]$ dBm. The normalized achievable data rate is a figure of merit defined as the ratio between the achievable data rate of OCFDM to that of OFDM. Moreover, we employed an SDP solver to obtain the OA for the cSNR case and the waterfilling for the uSNR.[1] First, under UA, it is noteworthy that the achievable data rate obtained with cSNR for OCFDM matched that of OFDM, becoming independent of the geometry. In fact, both the uniform and 32-geometry scenarios yielded the same data rate as OFDM, as confirmed in Fig. 3(a), where $\widehat{R} = 1$, $\forall P_{\mathrm{T}}$. This behavior contrasts with the findings in [7], where the geometry played a significant role in determining the data rate performance under uSNR. Focusing now on the achievable data rate under OA, the results reflected a familiar behavior, in which the geometry influences performance. In this case, OCFDM with uniform geometry outperformed the system with 32-geometry overall, achieving $\widehat{R} > 0.9$ for all values of P_{T}. In contrast, the 32-geometry configuration resulted in $\widehat{R} < 0.9$ for $P_{\mathrm{T}} \in [2, 7]$ dBm. These numerical findings highlight the potential of leveraging the correlation among chirps to enhance the achievable data rate.

Fig. 4 shows the OA power distribution across chirps for $P_{\mathrm{T}} = 7$ dBm. Although using the same multiplexing modulation technique, the allocated power was distributed differently for each geometry. This indicates that the method used to

[1] In OFDM systems, there is no cSNR case.

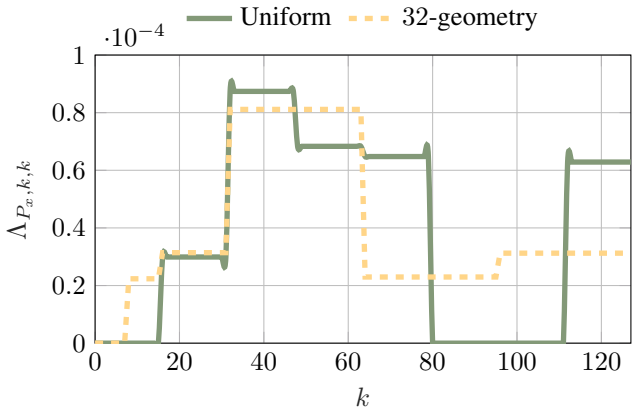

Fig. 4: Allocated power per chirp for Uniform geometry and 32-geometry when $P_{\mathrm{T}} = 7$ dBm.

group subcarriers into voices is a determining factor in maximizing the achievable data rate. Furthermore, it was observed that, for both techniques, the power was evenly distributed among chirps within the same voice, mirroring the behavior previously reported for the uSNR case—see Section IV-B of [7].

Overall, the numerical results provided important insights. Firstly, when UA was applied under cSNR, the achievable data rate became independent of geometry variations and matched that of OFDM. In contrast, the geometry continued to influence the data rate when OA was employed, following the remarks of [7]. Secondly, OA in OCFDM under cSNR led to an equal power distribution among chirps within the same voice, whereas the power allocation across different voices could vary. This result is consistent with the scenario in which chirp correlations are disregarded.

V. Conclusion

This paper presented an introductory study on the potential benefits of exploiting the correlations among different chirps within the same voice in OCFDM systems. To this end, we first provided a brief overview of the OCFDM system model, along with key concepts such as geometry and DMCT. Subsequently, we derived the expressions for the post-processing received signal, from which the cSNR matrix and the corresponding achievable data rate expression were obtained. Lastly, we demonstrated that the achievable data rate is concave with respect to the power assigned to each chirp, allowing for efficient numerical optimization through algorithms such as SDP. The achievable data rate for OCFDM under cSNR was evaluated for two geometries and two power-allocation strategies, namely OA and UA. The resulting data rates were then compared with previously reported results obtained under uSNR for both OCFDM and OFDM, using identical geometry and power-allocation conditions.

In future steps of this work, the implications of exploiting the correlated terms of chirps within their voices will be investigated in more practical scenarios, aiming to improve the bit-error probability for different modulations. More specifically, the investigation will focus on optimal decoders that consider chirp correlations and their relation to the achievable data rate of discrete constellations.

References

[1] P. S. R. Diniz, W. A. Martins, and M. V. S. Lima, *Block Transceivers: OFDM and Beyond*. San Rafael, CA: Morgan & Claypool, 2012.

[2] X. Ouyang and J. Zhao, "Orthogonal chirp division multiplexing," *IEEE Trans. Commun.*, vol. 64, no. 9, pp. 3946–3957, Sep. 2016.

[3] W. A. Martins, F. Cruz–Roldán, M. Moonen, and P. S. R. Diniz, "Intersymbol and intercarrier interference in OFDM transmissions through highly dispersive channels," in *Proc. 27th Eur. Signal Process. Conf. (EUSIPCO), A Coruña, Spain*, Sep. 2019, pp. 1–5.

[4] M. S. Omar and X. Ma, "Performance analysis of OCDM for wireless communications," *IEEE Trans. Wirel. Commun.*, vol. 20, no. 7, pp. 4032–4043, July 2021.

[5] T. F. Moreira, Â. Camponogara, S. Baig, and M. V. Ribeiro, "Performance analysis of orthogonal multiplexing techniques for PLC systems with low cyclic prefix length and symbol timing offset," *Sensors*, vol. 23, no. 9, Apr. 2023.

[6] M. S. Omar and X. Ma, "Designing OCDM-based multi-user transmissions," in *Proc. IEEE Glob. Commun. Conf. (Globecom), Waikoloa, USA*, Dec. 2019, pp. 1–6.

[7] T. F. Moreira, M. de L. Filomeno, W. A. Martins, and M. V. Ribeiro, "Orthogonal chirp-frequency division multiplexing," *IEEE Trans. Commun.*, vol. 73, no. 7, pp. 4630–4646, 2025.

[8] ——, "A frequency division modulation for CSS-based communication systems: An initial discussion," in *Proc. Symp. Internet Things (SIoT), São Paulo, Brazil*, Oct. 2023, pp. 1–5.

[9] P. P. Vaidyanathan, S.-M. Phoong, and Y.-P. Lin, *Signal processing and optimization for transceiver systems*. Cambridge, England: Cambridge University Press, Mar. 2010.

[10] S. Boyd and L. Vandenberghe, *Convex Optimization*. Cambridge, England: Cambridge University Press, Aug. 2016.

[11] L. Vandenberghe and S. Boyd, "Semidefinite programming," *SIAM Rev. Soc. Ind. Appl. Math.*, vol. 38, no. 1, pp. 49–95, Mar. 1996.

[12] A. Saleh and R. Valenzuela, "A statistical model for indoor multipath propagation," *IEEE J. Sel. Areas Commun.*, vol. 5, no. 2, pp. 128–137, Feb. 1987.

[13] *Wireless LAN Medium Access Control (MAC) and Physical Layer (PHY) Specifications*. IEEE Std. 802.11ax, 2021.

[14] N. Cravo, M. de L. Filomeno, and M. V. Ribeiro, "Hybrid power line/wireless systems: Analyses of normalized SNRs for in-home broadband scenarios," in *Proc. XL Simpósio Brasileiro de Telecomunicações e Processamento de Sinais, Santa Rita do Sapucaí, Brazil*, Sep. 2022, pp. 1–5.